

Experimental study of the wall boundary layer in Pb and Pb-Bi systems

Kirill Makhov, Aleksander Beznosov, Tatyana Bokova, Artem Shumilkov
makhov.87@inbox.ru beznosov@nntu.nnov.ru tatabo@bk.ru

Nizhny Novgorod State Technical University

Introduction

One of the most relevant problems includes endurance of steels when they are continuously in contact with a HLMC flow. Main efforts exerted by specialists in this field are focused on mechanistic studies of formation, destruction and properties of oxide coatings, depending both on structural material properties and on physical-chemical and thermohydraulic characteristics of high-temperature lead and Pb-Bi flows.

Corrosive wear is not the only one type of surface deterioration in a HLMC medium [1]. In bearing units, pump impellers operating in a HLMC medium, in the system "absorber element shell - casing" of the reactor core control and protection system and in the fuel element contact assembly in the spacer grid operating in a HLMC medium, the following mechanisms may be implemented:

- abrasive wear caused by the effect of solid impurity particles;
- cavitation wear of circulation pump impellers ;
- breaking-out of metal;
- plastic deformation;
- other mechanisms [2].

Handling problems for substantiating material durability in a HLMC medium is complicated by the fact that lead and lead-bismuth coolants cannot be regarded as those having a complete set of medium lubrication properties due to:

- low (as compared with conventional lubricants) viscosity;
- unwettability of surfaces if there are oxide coatings;
- a high heat removal rate from friction units [3]

1. A.V. Nazarov. Research of Contact Component Interaction Performance of Mechanisms in a High-Temperature Lead and Lead-Bismuth Coolant Medium: Ph.D. Thesis in Engineering Science: April 5, 2011 / Anton Anatolievich Molodtsov. – N. Novgorod, 2007.

2. Types of Wear of Contact Surfaces in High-Temperature Lead and Lead-Bismuth Coolants // A.V. Beznosov, T.A. Bokova, M.A. Antonenkov, K.A. Makhov, Yu.N. Drozdov, V.V. Makarov, V.N. Puchkov / Nuclear Power. 2009. Vol. 107. No. 5. P. 252-258.

3. A.V. Beznosov. Equipment of Power Circuits Using Heavy Liquid-Metal Coolants in Nuclear Power Industry / A.V. Beznosov, T.A. Bokova; Nizhny Novgorod State Technical University n.a. R.E. Alekseyev. – Nizhny Novgorod, 2012. – p. 536: Fig.

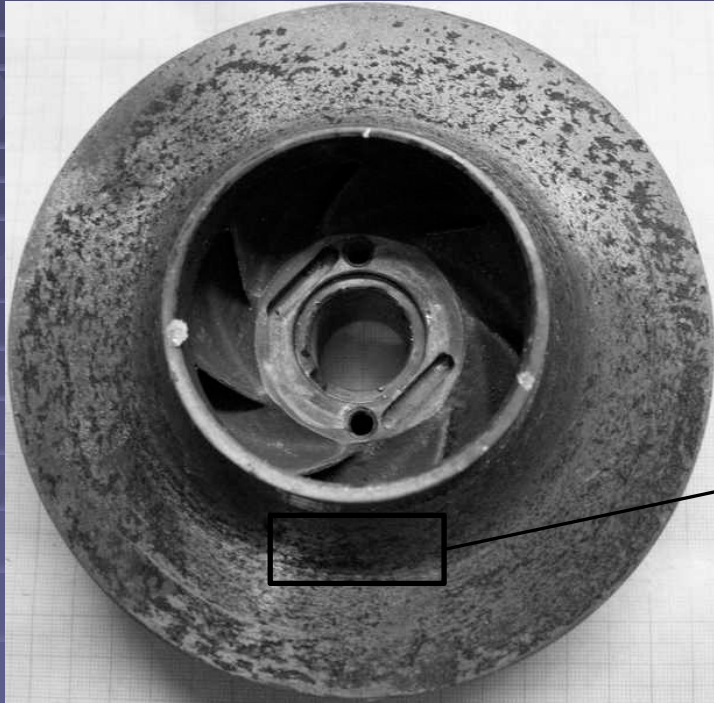


a)

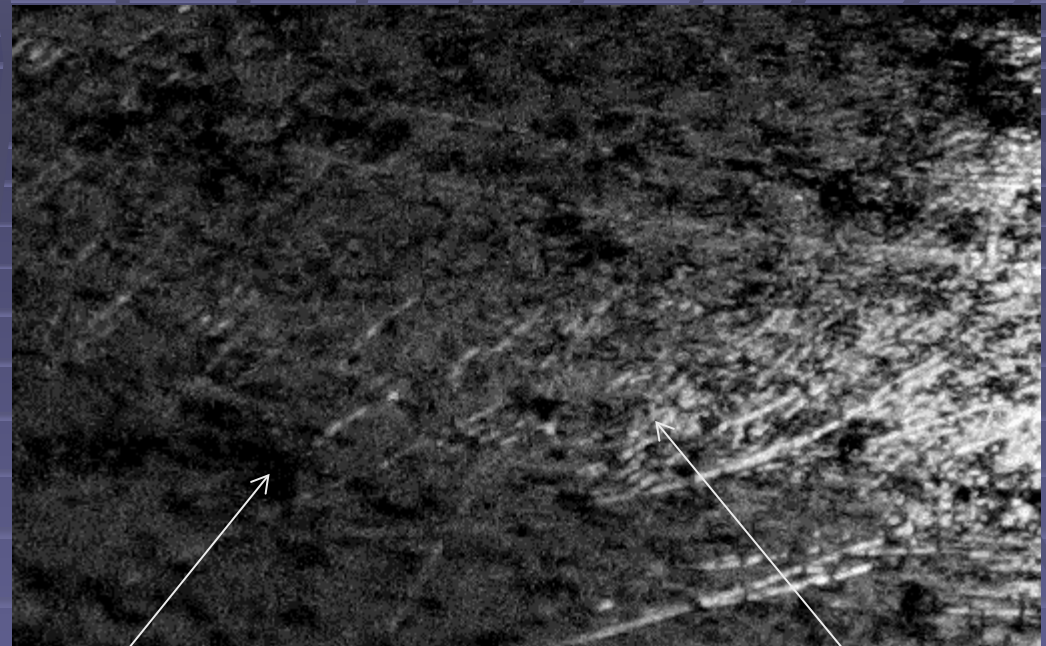


b)

Pictures of a bearing sleeve (a) – steel 40Cr13 (diameter 32 mm, tolerance plus 0.55 ... 0.6 mm) and a shaft neck (b) – steel 12Cr18Ni10Ti (diameter 32 mm, tolerance b9) with scratch marks on dry-friction bearing surfaces of gas handler DG-03 following 80 hours of operation in a lead medium; experiment for the evaluation of the structure of two-phase lead-gas flows generated by centrifugal dispersers: lead temperature 450 ... 540 °C, shaft speed 600 ... 3,000 rpm, thermodynamic activity of oxygen in lead 10^{-5} ... 10^0 .



a)

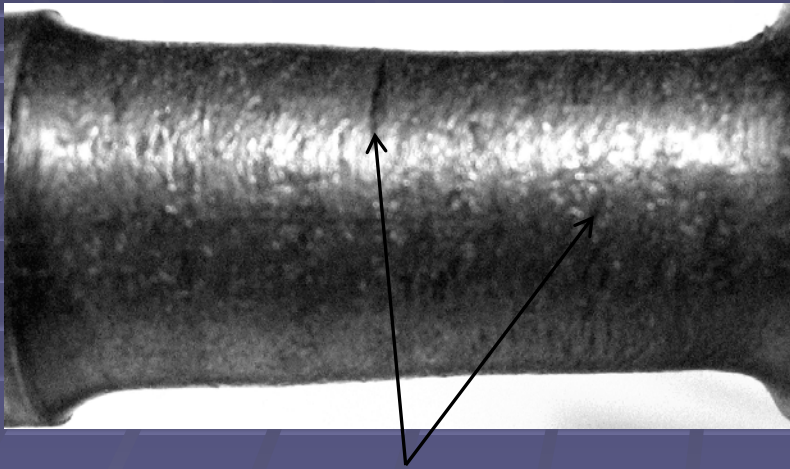


1

2

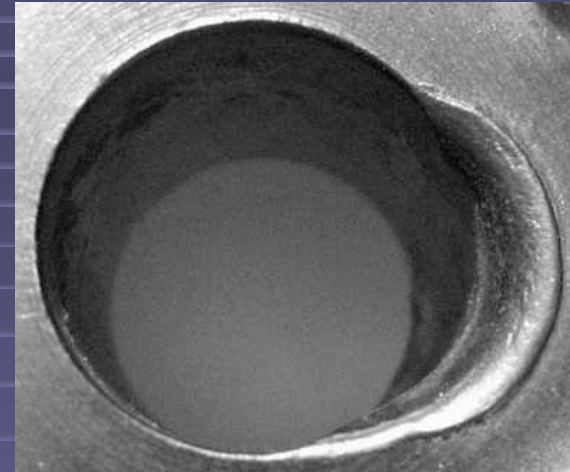
b)

Picture of a centrifugal wheel (a) and a cover disk area (b) of centrifugal pump NTsS-04 with signs of corrosive (1) and abrasive (2) wear: pumped lead temperature 350 ... 510 °C, thermodynamic activity of oxygen in lead 10^{-5} ... 10^0 , maximum peripheral speed 12 m/s, time in service 1,670 hours



Breaking-out of metal

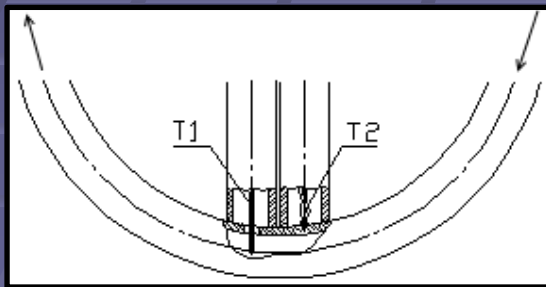
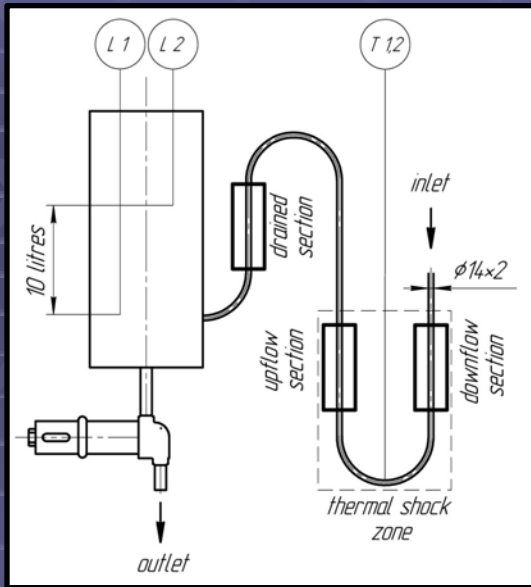
Picture of a gearbox wheel dry-friction bearing shaft neck having signs of bursts on the bearing surface following 7 hours of operation in a lead medium: lead temperature 450 °C, shaft speed 1,500 rpm, thermodynamic activity of oxygen in lead on saturation line, shaft neck material – steel 12Cr18Ni10Ti, bearing sleeve material – steel 12Cr18Ni10Ti, neck diameter 15 mm and 10 mm before and after the experiment respectively



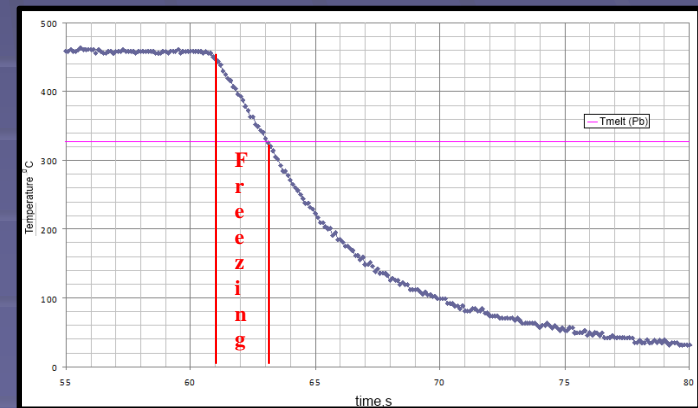
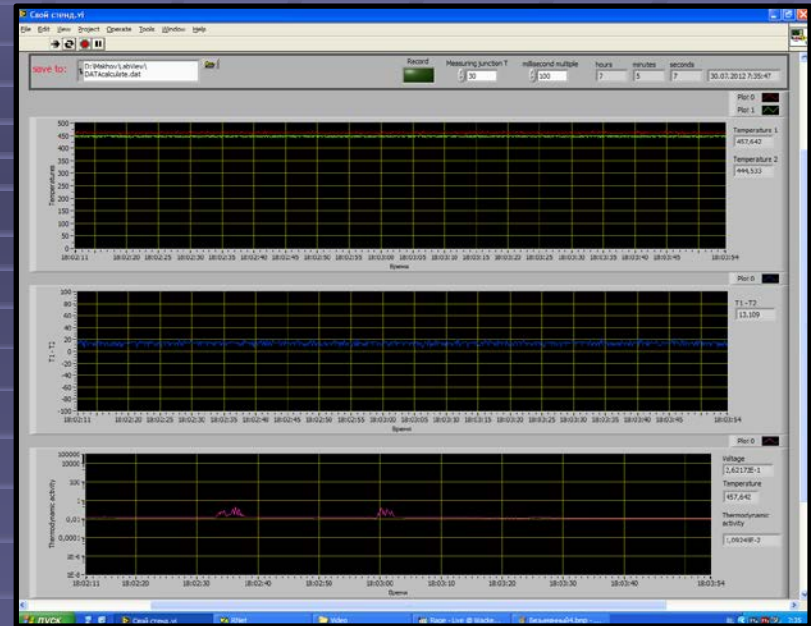
Picture of a gearbox wheel dry-friction bearing sleeve having signs of plastic deformation (dimpling) on the bearing surface following 7 hours of operation in a lead medium: lead temperature 450 °C, shaft speed 1,500 rpm, thermodynamic activity of oxygen in lead on saturation line, bearing sleeve material – steel 12Cr18Ni10Ti, shaft neck material – steel 12Cr18Ni10Ti

The work objective included:

- evaluating structures being formed in the wall boundary area where HLMC contacts the surfaces of structural materials;
- investigating effects of the circuit operating parameters on alteration of the wall boundary layer parameters (surface roughness) in a circulating HLMC medium;
- identifying contact surface wear mechanisms and forces arising in the isolated situation of the system model "neutron absorber element shell – casing" as applied to the reactor core control and protection system conditions.



Test Section Diagram



| Type | Chemical Composition | | | | | | | | |
|--------------|----------------------|------|--------|--------|------|-----------|----------|---------|--------|
| | C | Mn | P | S | Si | Cr | Ni | Ti | Others |
| 12Cr18Ni10Ti | ≤0.12 | ≤2.0 | ≤0.035 | ≤0.020 | ≤0.8 | 17.0~19.0 | 9.0~11.0 | 5·C-0.8 | Cu≤0.3 |

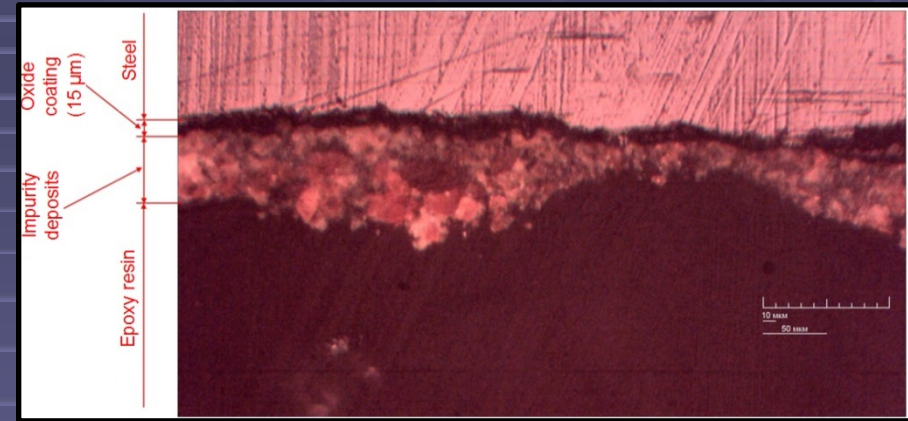
Experimental Conditions

IWSMT-12
19-23 October 2014
Bregenz, Austria

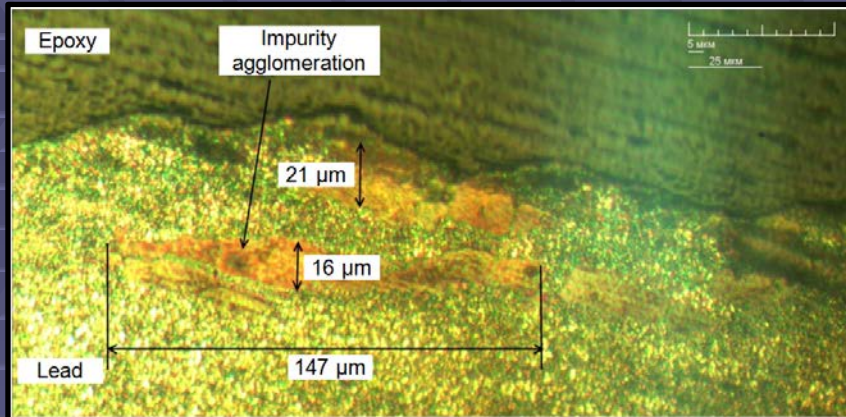
| Experiment Number | Type of Coolant | Initial Coolant Temperature, °C | Final Coolant Temperature, °C | Thermodynamic Activity of Oxygen | Circulation Time, h | Coolant Flow, m ³ /h | Mean Flow Velocity, m/s | Reynolds Number, Re |
|-------------------|-----------------------------------|---------------------------------|-------------------------------|-----------------------------------|---------------------|---------------------------------|-------------------------|-----------------------|
| 1 | Pb | 550 | 20 | 10 ⁰ -10 ⁻¹ | 100 | 0.55 | 2 | 1.074*10 ⁵ |
| 2 | Pb | 470 | 20 | 10 ⁻³ | 50 | 0.27 | 1 | 5.394*10 ⁴ |
| 3 | Pb | 470 | 20 | 10 ⁻³ | 75 | 0.27 | 1 | 5.394*10 ⁴ |
| 4 | Pb | 450 | 20 | 10 ⁻² | 22 | 0.27 | 1 | 5.394*10 ⁴ |
| 5 | Pb | 450 | 20 | 10 ⁻² | 32 | 0.27 | 1 | 5.394*10 ⁴ |
| 6 | Pb ₄₅ Bi ₅₅ | 400 | 20 | 10 ⁻³ | 50 | 0.4 | 1.4 | 7.55*10 ⁴ |
| 7 | Pb ₄₅ Bi ₅₅ | 400 | 20 | 10 ⁻³ | 75 | 0.4 | 1.4 | 7.55*10 ⁴ |
| 8 | Pb ₄₅ Bi ₅₅ | 400 | 20 | 10 ⁻³ | 75 | 0.4 | 1.4 | 7.55*10 ⁴ |
| 9 | Pb ₄₅ Bi ₅₅ | 400 | 20 | 5*10 ⁻⁴ | 75 | 0.4 | 1.4 | 7.55*10 ⁴ |
| 10 | Pb ₄₅ Bi ₅₅ | 350 | 20 | 10 ⁻³ | 75 | 0.4 | 1.4 | 7.55*10 ⁴ |
| 11 | Pb ₄₅ Bi ₅₅ | 400 | 20 | 10 ⁻³ | 75 | 0.255 | 0.9 | 4.9*10 ⁴ |
| 12 | Pb ₄₅ Bi ₅₅ | 400 | 20 | 10 ⁻³ | 75 | 0.14 | 0.5 | 2.7*10 ⁴ |



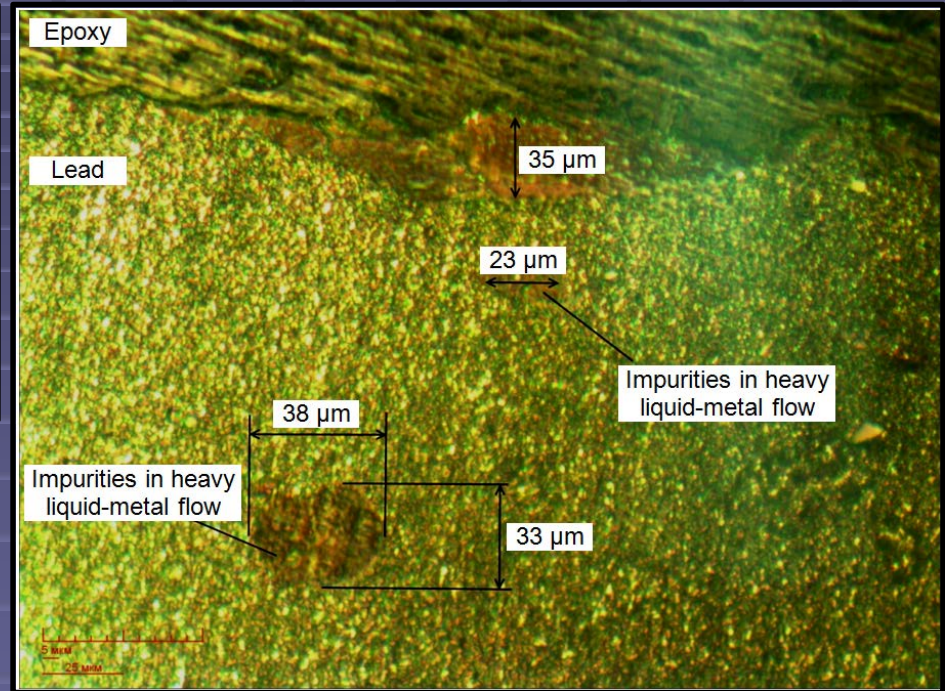
Picture of Sample Wall Boundary Area ($T= 550^{\circ}\text{C}$, $t=100$ hours, $a=10^{-1}-10^0$, $Q=0.55$ m³/h, $V=2$ m/s, $Re=1.074*10^5$) at 200-Fold Magnification



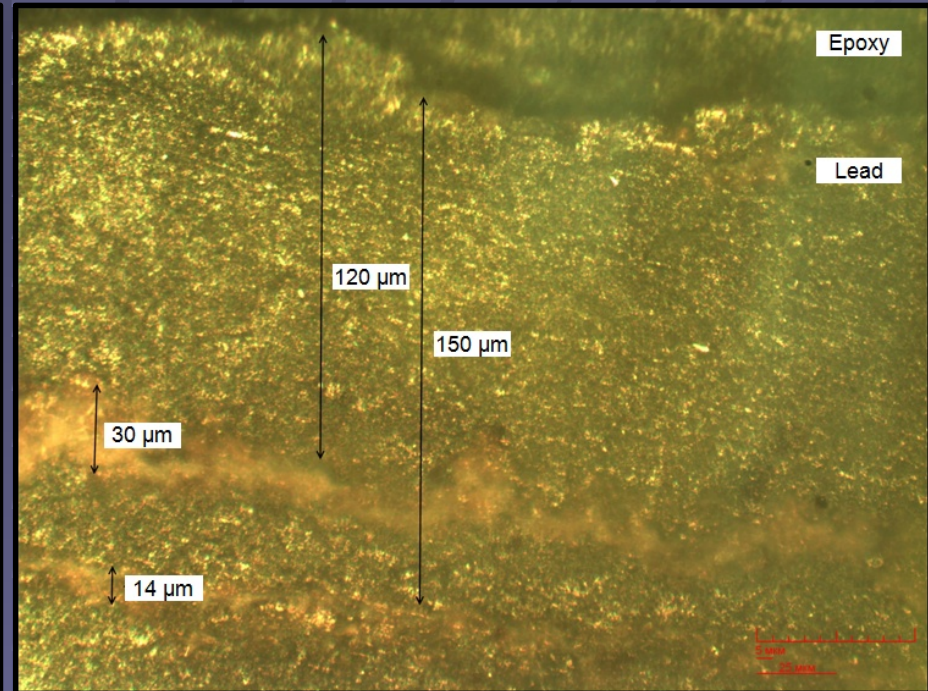
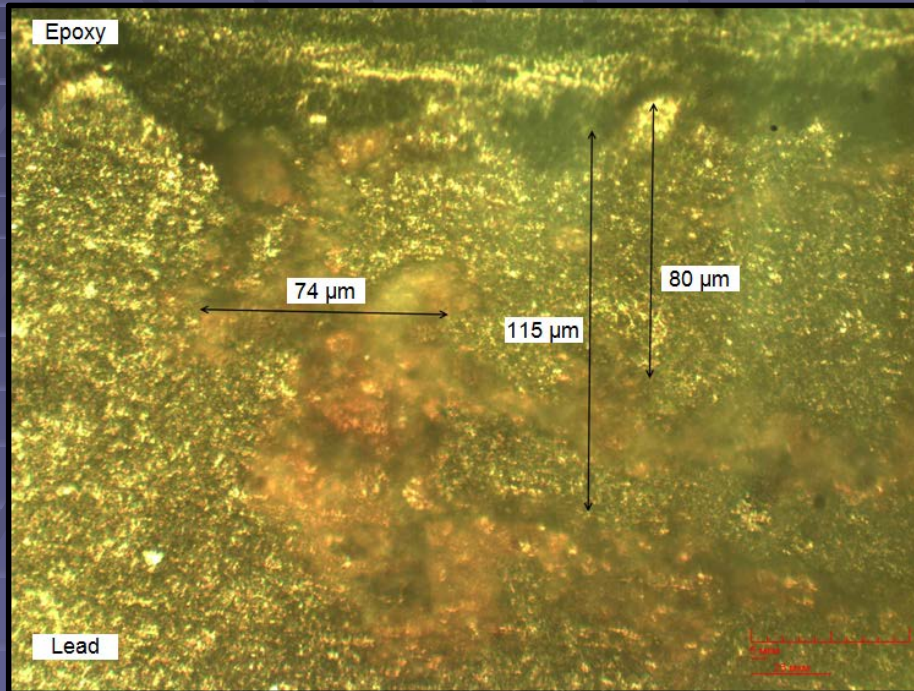
Impurity Conglomerates Remaining After Separation of Lead Ingot on Steel Surface ($T= 550^{\circ}\text{C}$, $t=100$ hours, $a=10^{-1}-10^0$, $Q=0.55$ m³/h, $V=2$ m/s, $Re=1.074*10^5$) at 200-Fold Magnification



Impurity Conglomerates Remaining After Separation of Lead Ingot in Hardened Lead Flow ($T= 470^{\circ}\text{C}$, $t=50$ hours, $a=10^{-3}$, $Q=0.27$ m³/h, $V=1$ m/s, $Re=5.394*10^4$) at 400-Fold Magnification in Scope of "Frozen" Lead Flow



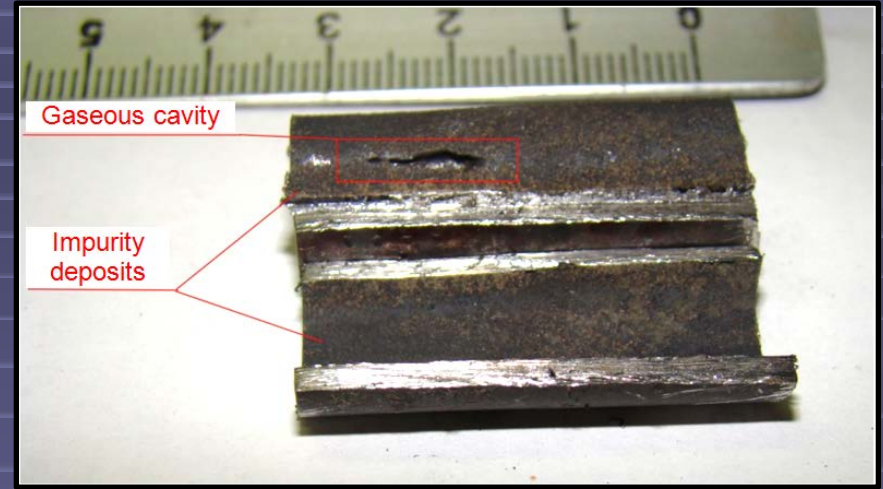
Formations of Impurity Particles Saturated with Lead ($T= 470^{\circ}\text{C}$, $t=50$ hours, $a=10^{-3}$, $Q=0.27$ m³/h, $V=1$ m/s, $Re=5.394*10^4$) at 400-Fold Magnification in Scope of "Frozen" Lead Flow



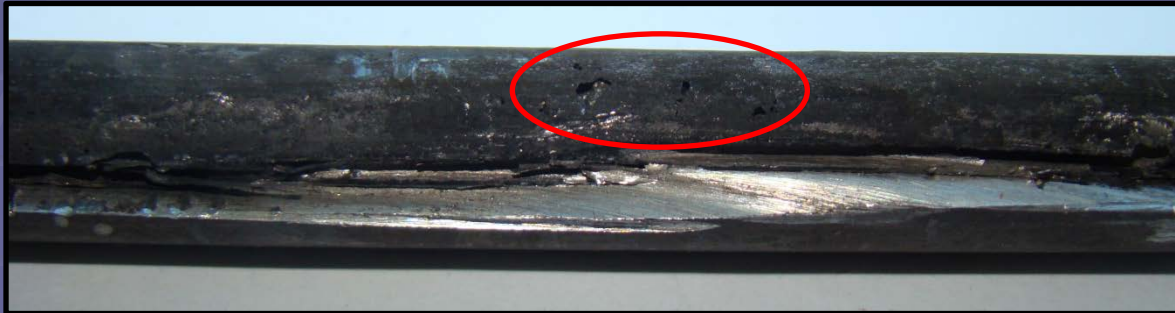
Impurity Conglomerates Remaining After Separation of Lead Ingot in Hardened Lead Flow ($T= 470^{\circ}\text{C}$, $t=32$ hours, $a=10^{-2}$, $Q=0.27\ \text{m}^3/\text{h}$, $V=1\text{m/s}$, $Re=5.394*10^4$) at 400-Fold Magnification in Scope of "Frozen" Lead Flow



Gaseous (Gas-Vapor) Cavity in Lead Ingot
($T= 450^{\circ}\text{C}$, $t=22$ hours, $a=10^{-2}$, $Q=0.27$ m³/h,
 $V=1\text{m/s}$, $\text{Re}= 5,394*10^4$)

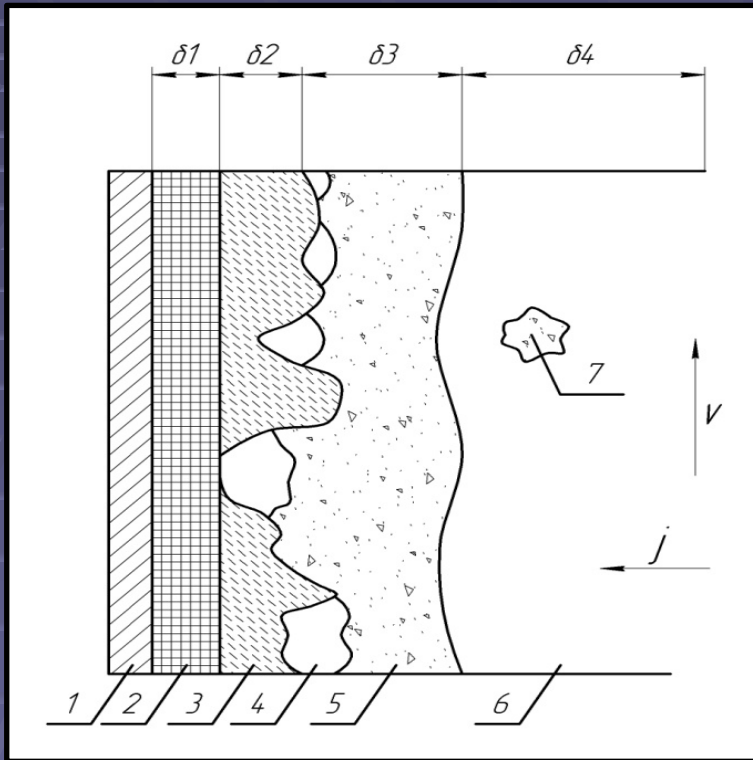


Gaseous (Gas-Vapor) Cavity in Lead Ingot
($T= 550^{\circ}\text{C}$, $t=100$ hours, $a=10^{-1}-10^0$, $Q=0.55$ m³/h,
 $V=2\text{m/s}$, $\text{Re}=1.074*10^5$)

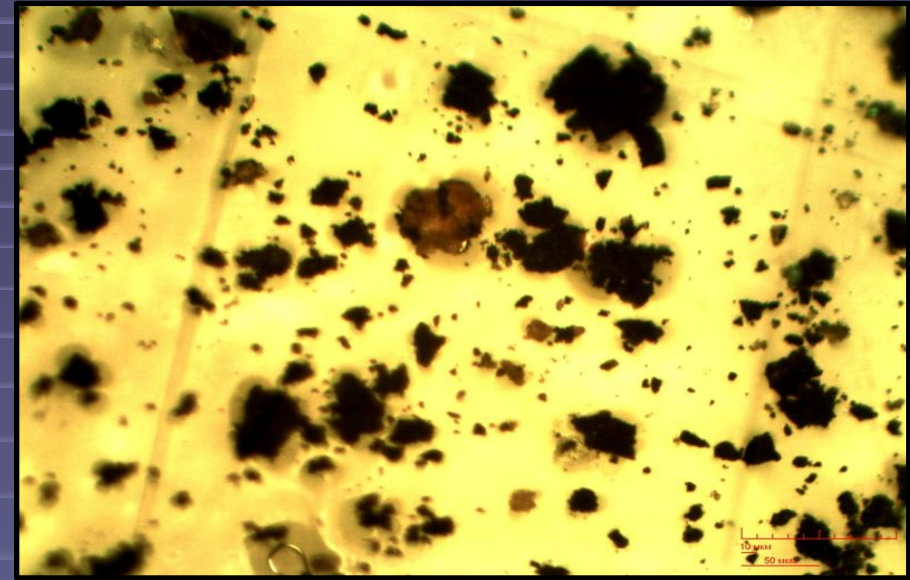


Gaseous (Gas-Vapor) Cavity in Lead-Bismuth Ingot
($T= 400^{\circ}\text{C}$, $t=75$ hours, $a=10^{-3}$,
 $Q=0.27$ m³/h, $V=1\text{m/s}$, $\text{Re}= 5,394*10^4$)

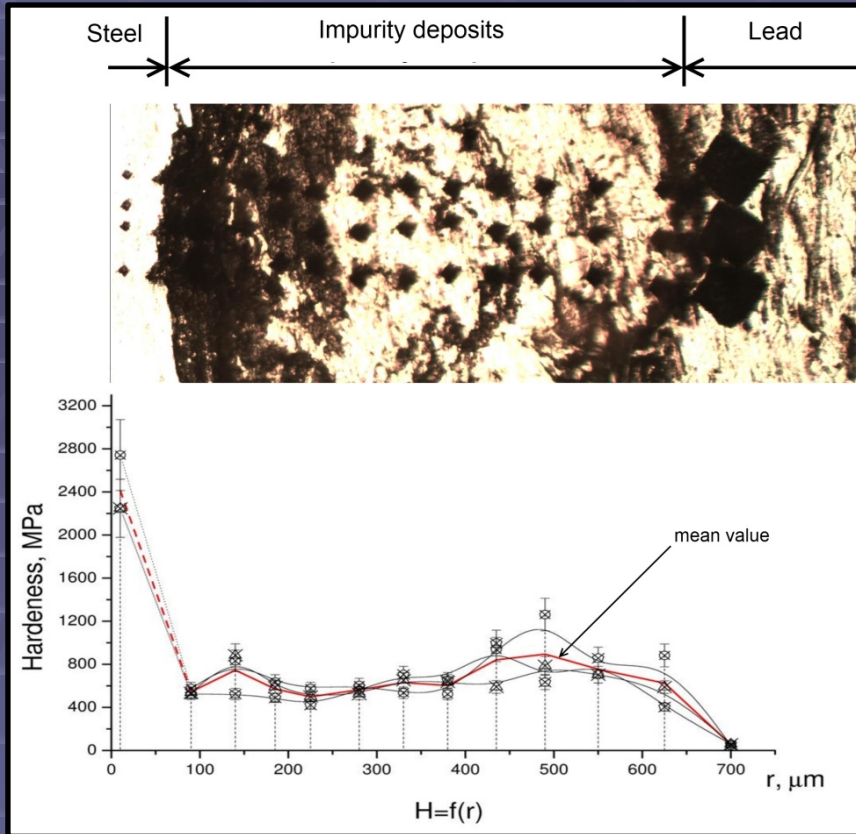
Diagram of Wall Boundary Area of Solid and Liquid Metal Contact



- 1 – steel;
- 2 – oxide coating;
- 3 – layer of friable deposits weakly bonded with oxide coating;
- 4 – gaseous phase (due to unwettability of oxide coating with coolant);
- 5 – diffusion layer of boundary turbulent layer enriched with impurities;
- 6 – boundary turbulent layer;
- 7 – impurity particles located in coolant flow near wall boundary area 5.



Picture of impurity particles at 200-fold magnification under the microscope (average particle area $\approx 120 \mu\text{m}^2$, at relative filling of photographically recorded area $\approx 20\%$)



Testing Results for Micro-Hardness of Wall Boundary Area After Express Freezing of Lead Flow ($T=550^{\circ}\text{C}$, $t=100$ hours, $a=10^{-1}-10^0$, $Q=0.55$ m^3/h , $V=2\text{m}/\text{s}$, $\text{Re}=1.074 \cdot 10^5$)

Tester: Shimadzu HMV-2T;
Instrumental error: 8-12%;
Load – 20g;
Exposure time – 10s

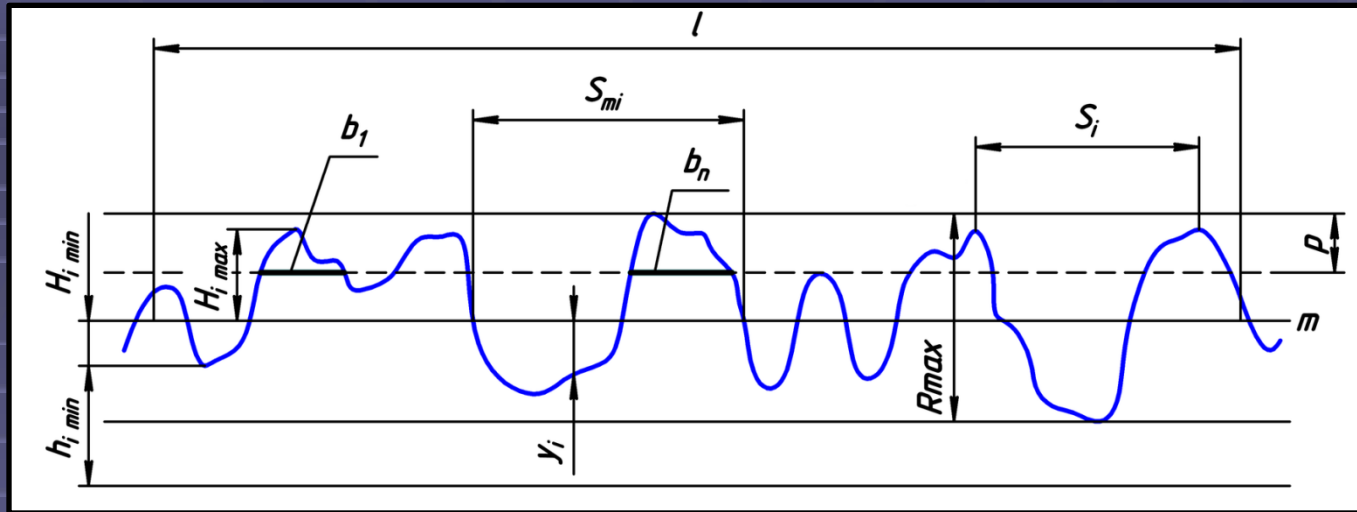
The ultimate composition of impurities:

Pb-80%;
 O_2 -7.5%;
Cr-0.01%;
Ni-0.01%;
Fe-0.1%;
Sb-0.1%;
Bi-0.7%;
Sn-0.5%;
C-0.1%.

X-ray method:

- Major phase – tetragonal modification of PbO (~75%);
- Cubic modification of Pb (~20%);
- The rest – impurities

Tester: Shimadzu XRD-6000 X-ray diffractometer (CuK_α -radiation, reflection exposure geometry);
Instrumental error: 10%;
Scanning pitch – 0.02Θ ;
Interval of 2Θ – $10 - 60^\circ$



$$R=f(T)_{a,t,V=\text{const}}$$

$$R=f(a)_{T,t,V=\text{const}}$$

$$R=f(t)_{a,T,V=\text{const}}$$

$$R=f(V)_{T,t,a=\text{const}}$$

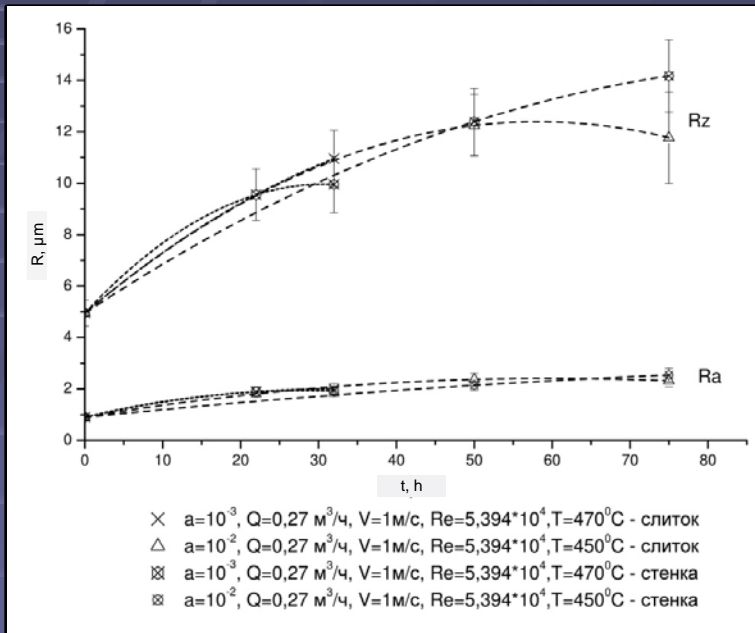
$$R=f(T,a,t,V(Q,Re))$$

$$R_a = \frac{1}{l} \int_0^l [y_i] dx$$

$$R_z = \left(\sum_{i=1}^n H_{i_{\max}} - \sum_{i=1}^n H_{i_{\min}} \right) / 5$$

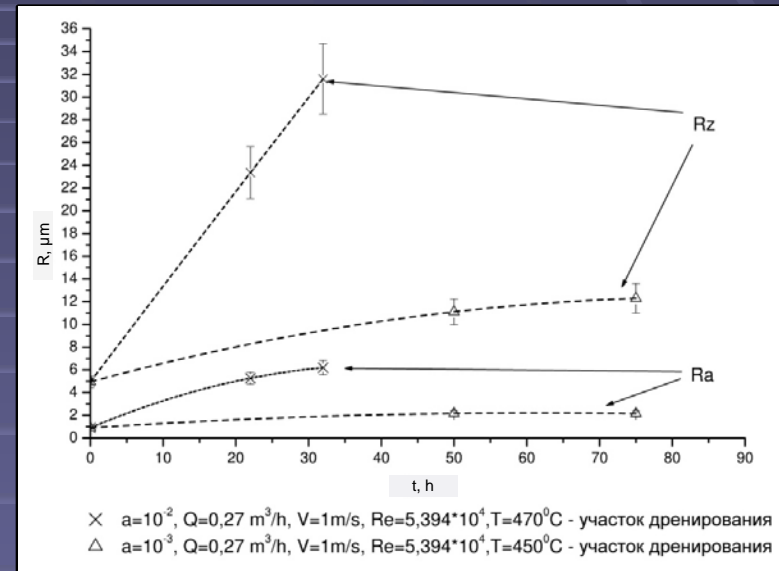
l – sampling length

Tester: TR220;
 Instrumental error: 10%;
 Sampling length – 8mm;
 Number of measurements (of each sample): 5



$R=f(t)$

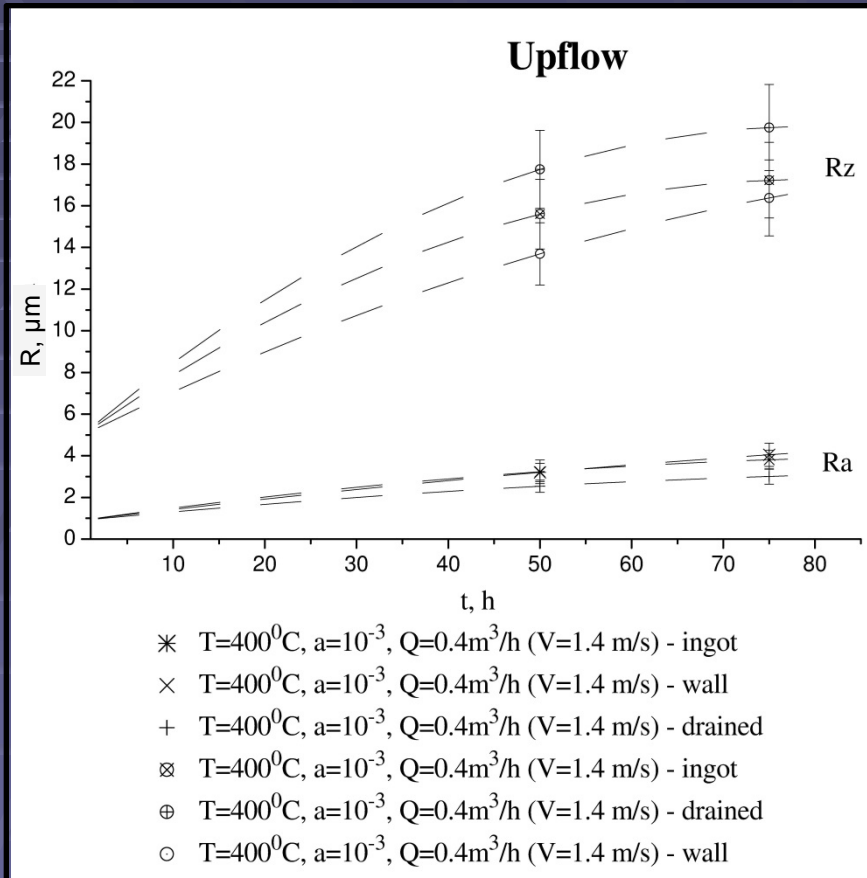
$$Ra=Ra_0+0.32\ln(t); Rz=Rz_0+1.64\ln(t)$$



$R=f(t)$

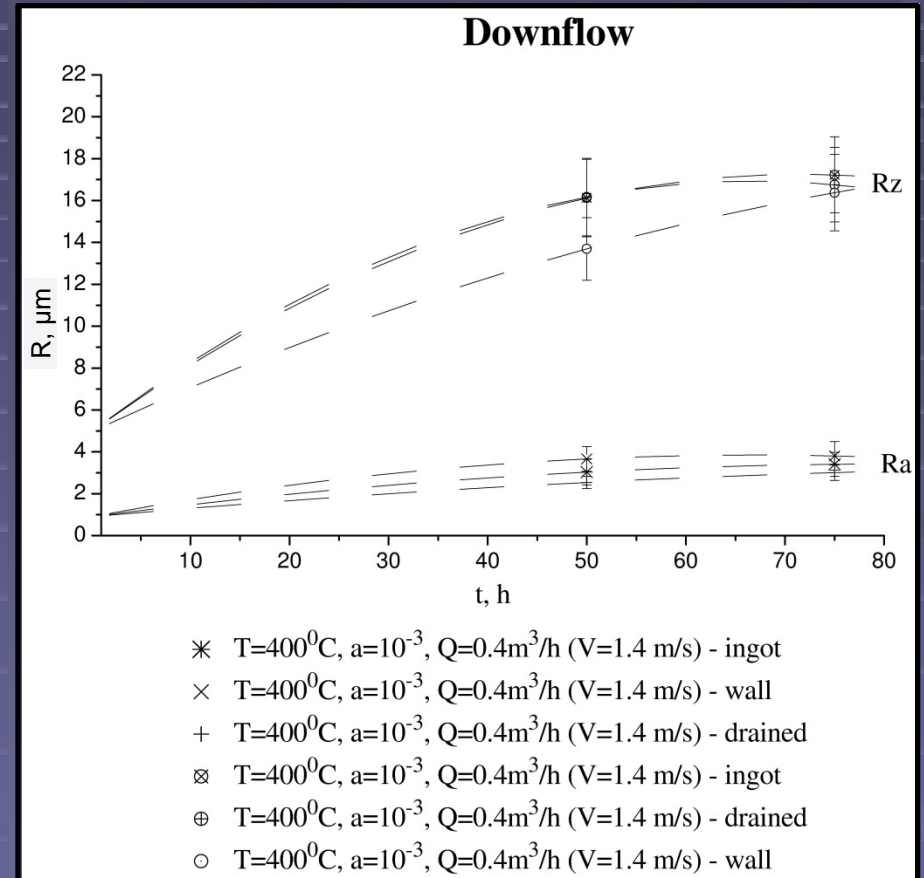
$$Ra=Ra_0+0.3\ln(t); Rz=Rz_0+1.7\ln(t)$$

$$Ra=Ra_0+1.5\ln(t); Rz=Rz_0+7\ln(t)$$



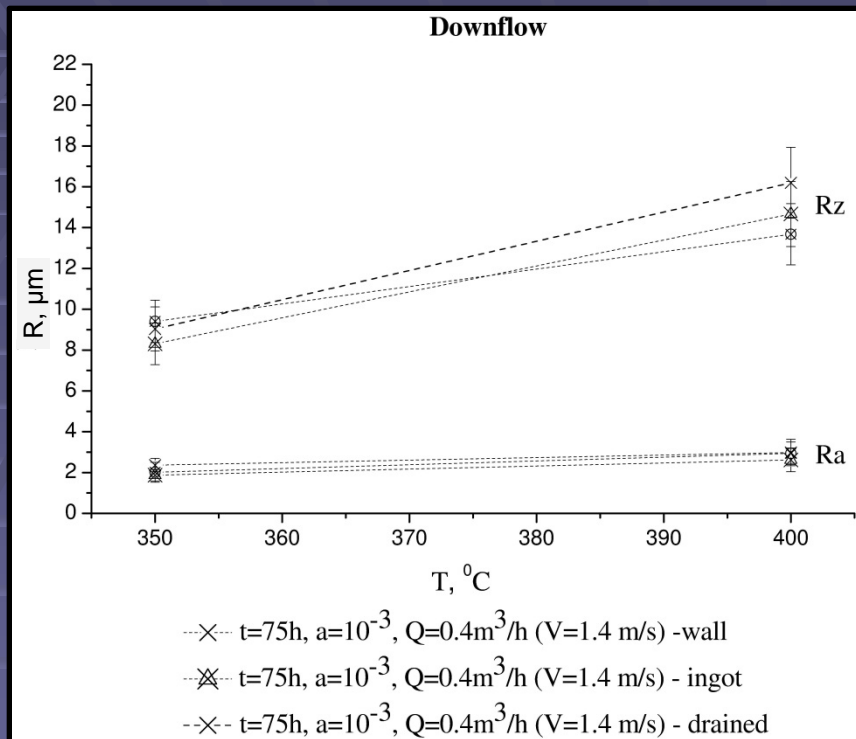
$R=f(t)$

$$Ra=Ra_0+0.67\ln(t); Rz=Rz_0+3.37\ln(t)$$

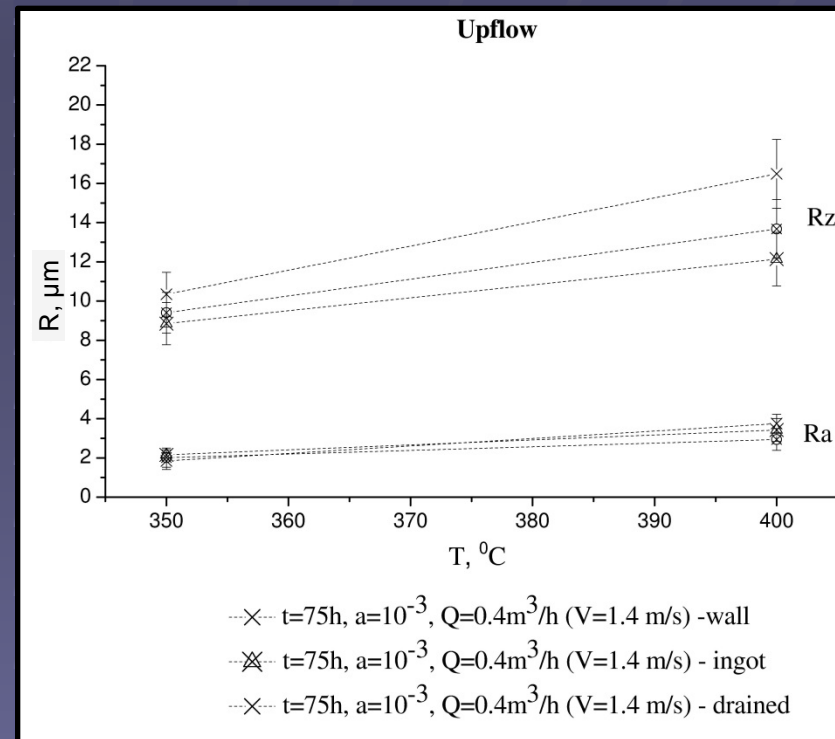


$R=f(t)$

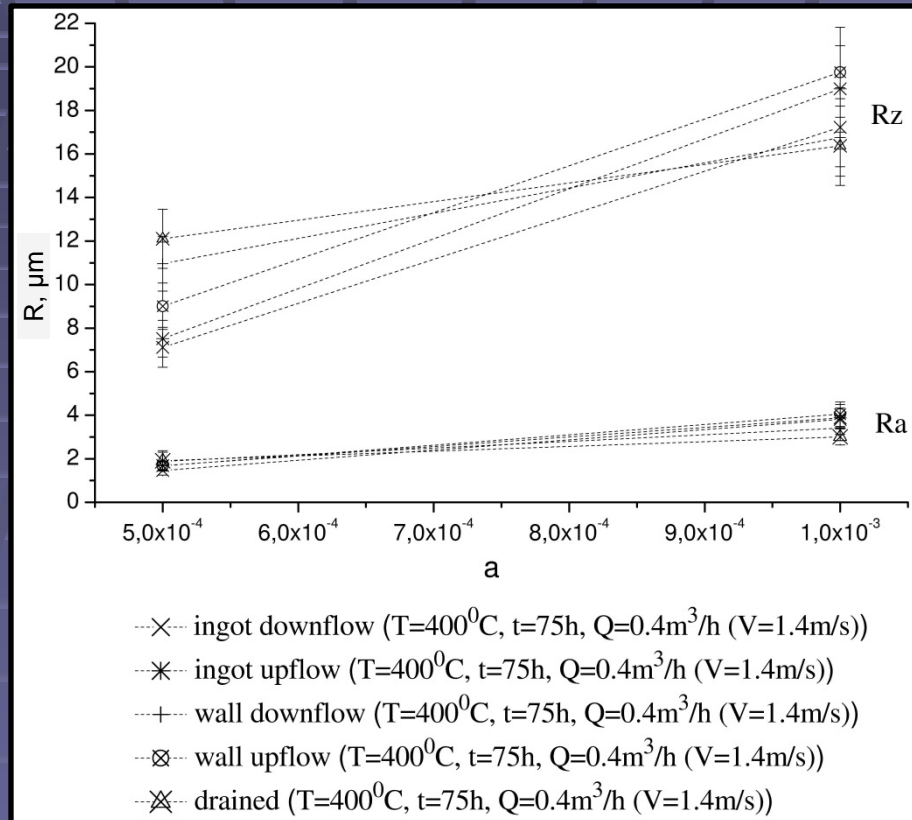
$$Ra=Ra_0+0.57\ln(t); Rz=Rz_0+2.79\ln(t)$$



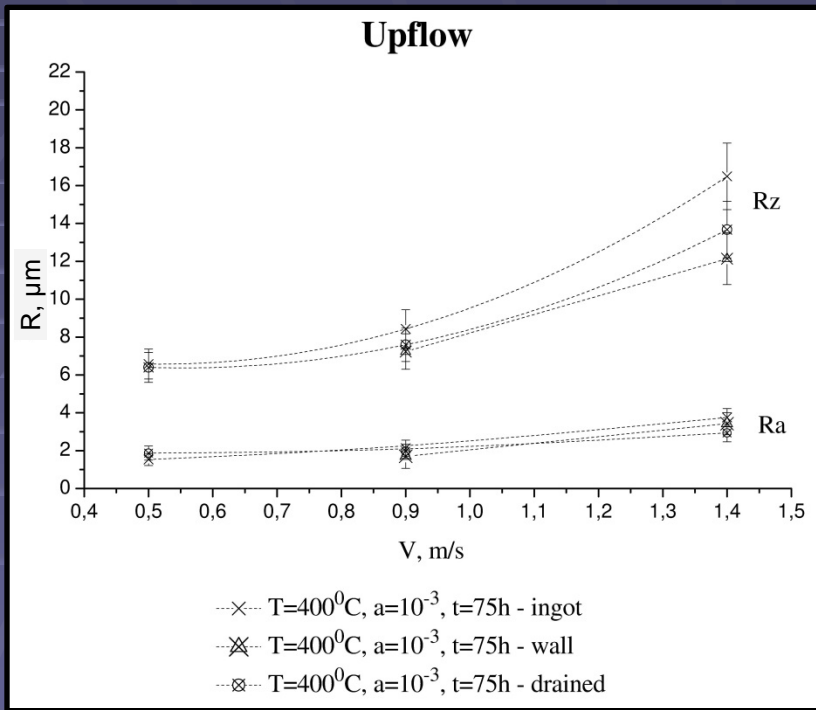
$R=f(T)$



$R=f(T)$



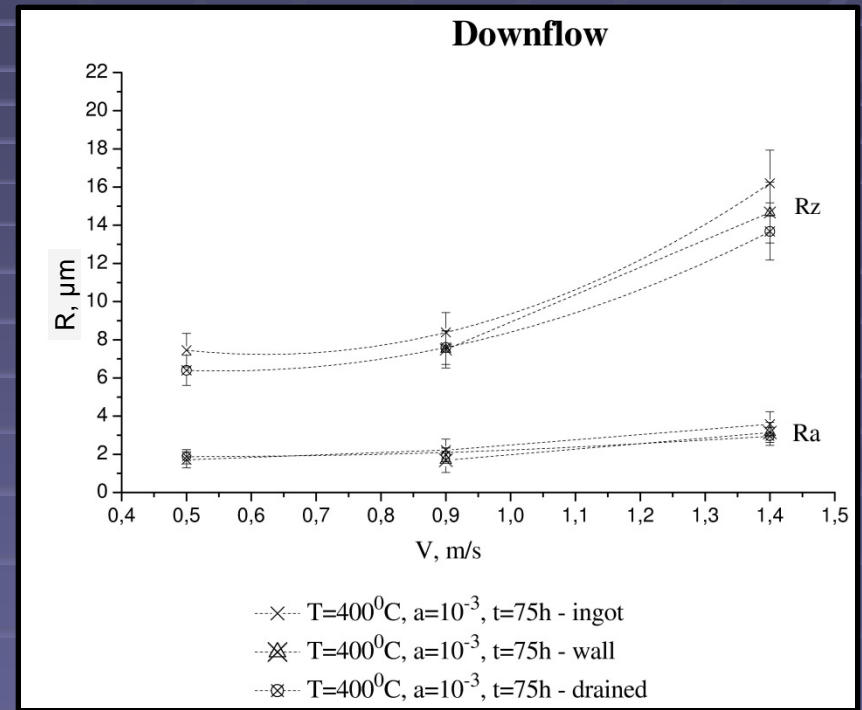
$$R=f(a)$$



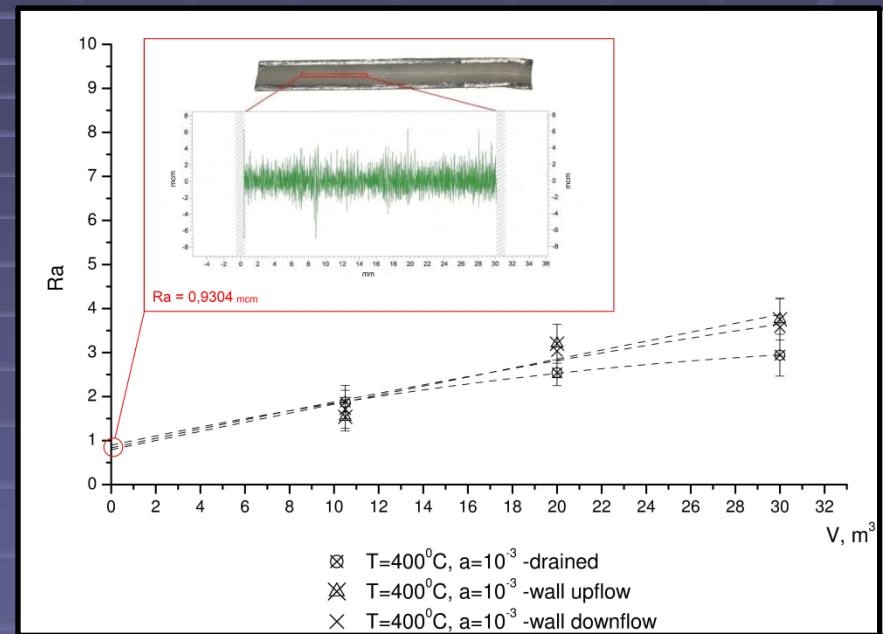
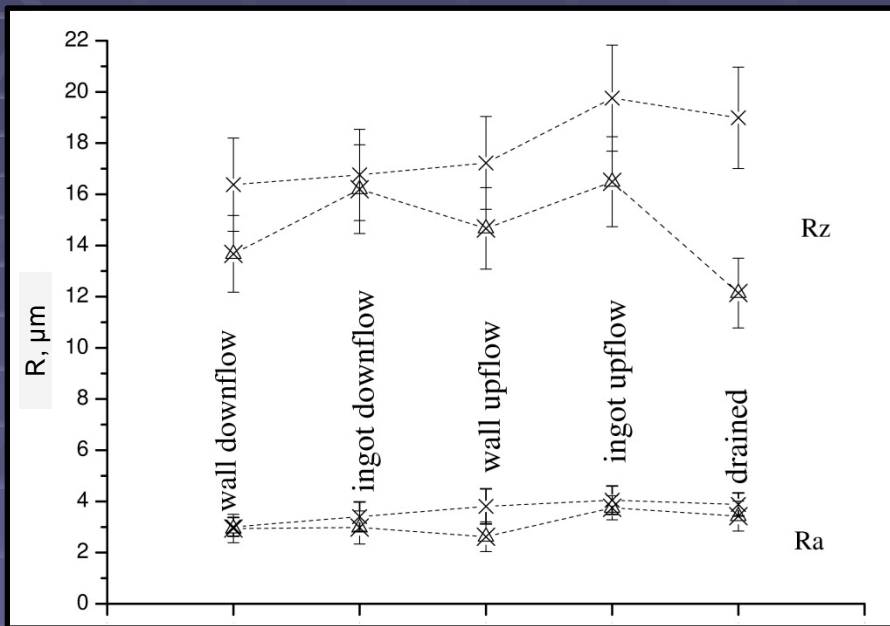
$$R=f(V)$$

$$R_a=R_{a_0} \cdot e^{\nu}$$

$$R_z=R_{z_0} \cdot e^{\nu}$$



$$R=f(V)$$



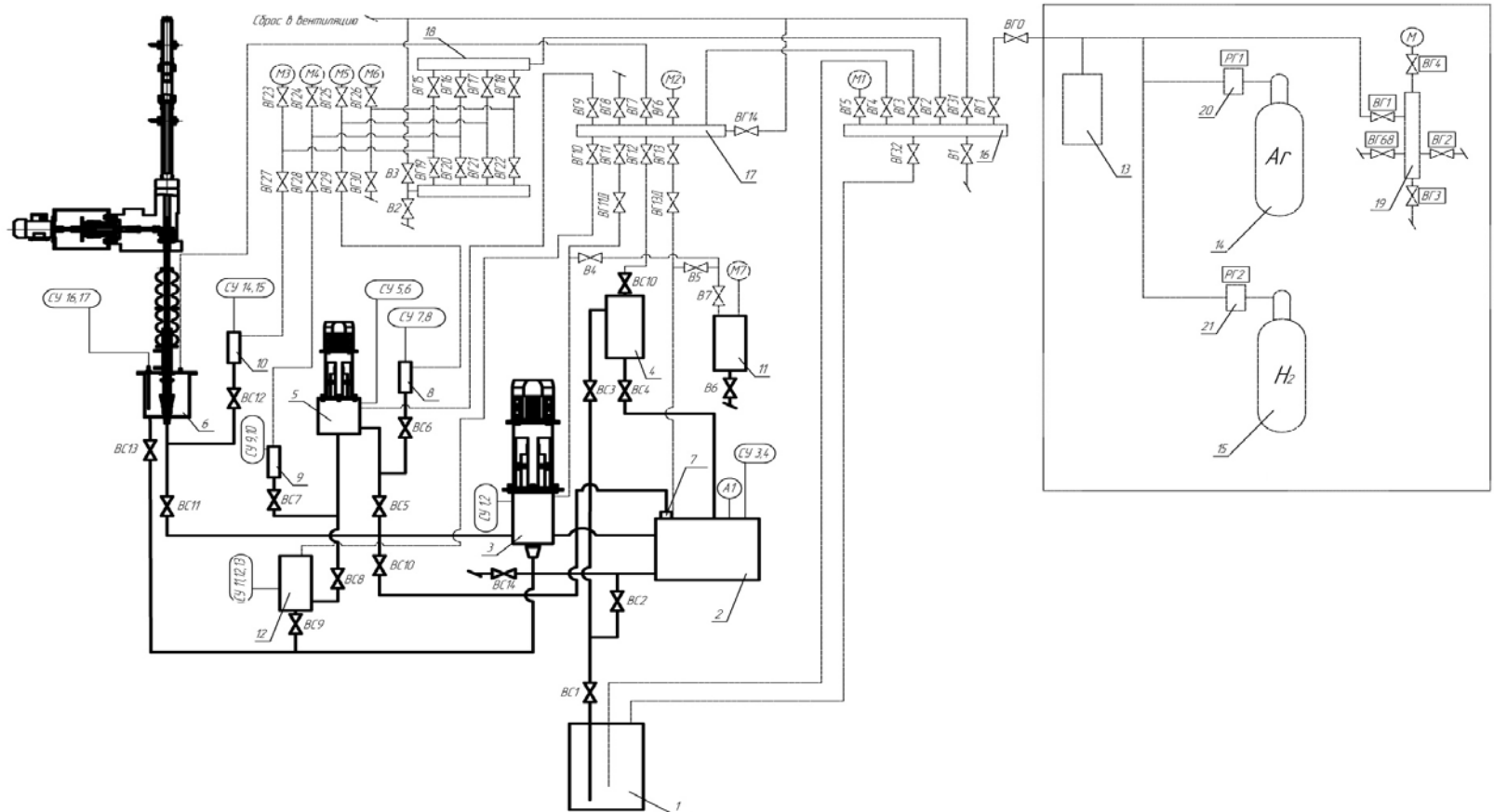
Comparison

$Q=0.4 \text{ m}^3/\text{h}$, $T=400^\circ\text{C}$, $a=10^{-3}$, $t=75\text{h}$

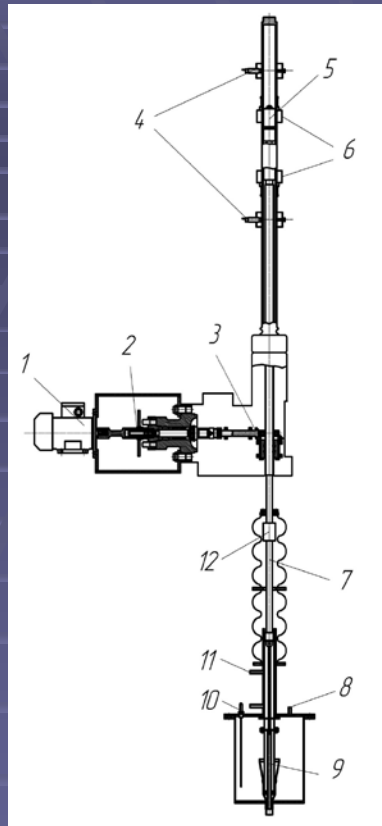
Circulating factor

$$\begin{aligned}
 Q &= v \cdot S \\
 Q &= \frac{V}{t}
 \end{aligned}
 \left. \vphantom{\begin{aligned} Q &= v \cdot S \\ Q &= \frac{V}{t} \end{aligned}} \right\} \rightarrow V = v \cdot S \cdot t$$

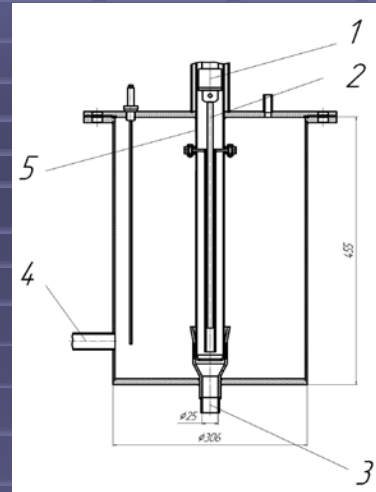
$Q, \text{ m}^3/\text{h} \text{ (m}^3/\text{s)}$
 $v, \text{ m/s}$
 $V, \text{ m}^3$
 $t, \text{ h(s)}$



1 – melting tank; 2 – buffer tank; 3 – HLHC pump; 4 – filter; 5 - experimental facility “bearing”; 6 - experimental facility “RCPS drive”; 7 – gas-mass exchanger; 8,9,10 - pressure measurement systems; 11 – condenser; 12 – flow rate meter; 13 – gas accumulating tank; 14 – Ar gas vessel; 15 – H₂ gas vessel; 16,17,18,19 - gas collectors; 20 – Ar pressure regulator; 21 - H₂ pressure regulator

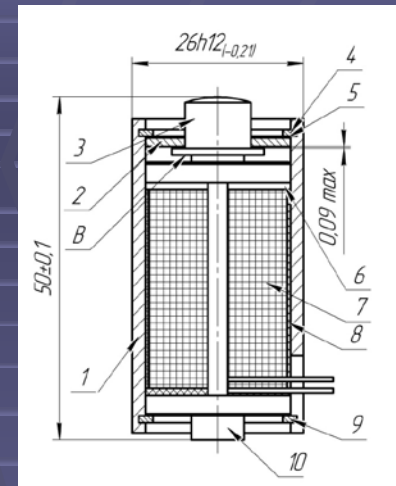


1 – electric motor; 2 – torque sensor; 3 – power transmission; 4 – top and bottom sealed contacts; 5 – magnet; 6 – terminal inductive switches (TIS); 7 – shaft; 8 – gas system nozzle; 9 – test section; 10 – conductivity level sensors; 11 – cooling body; 12 – magneto-elastic stress sensor



1 – gripping socket;
 2 – absorber rod simulator;
 3 – inlet nozzle;
 4 – outlet nozzle;
 5 – overflow outlets.

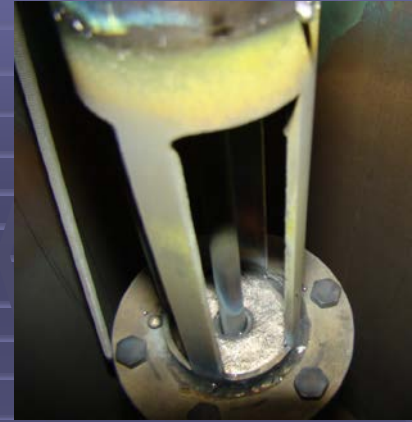
annular clearance -1 mm;
 lead temperature – 475-480°C;
 circulation time – 8 hours;
 rod rate of travel relative to cladding – 4 cm/s;
 coolant velocity in annular clearance – 1.2 m/s;
 thermodynamic activity of oxygen – 10^{-2}



Magneto-elastic stress sensor of the friction couple contact interaction force variation system "absorber rod simulator – cladding"

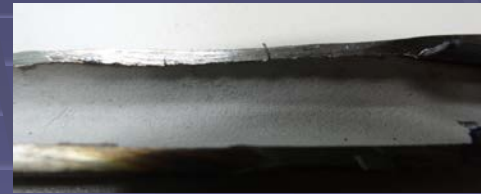


Test section diagram (top), appearance of experimental channel outlet section before (left) and after (right) experiment



Ra=0.812 μm , Rz=5.034 μm

State of surfaces before experimental research



Ra=1.624 μm , Rz=7.997 μm



Deterioration with destruction of oxide coatings and surface wetting with coolant

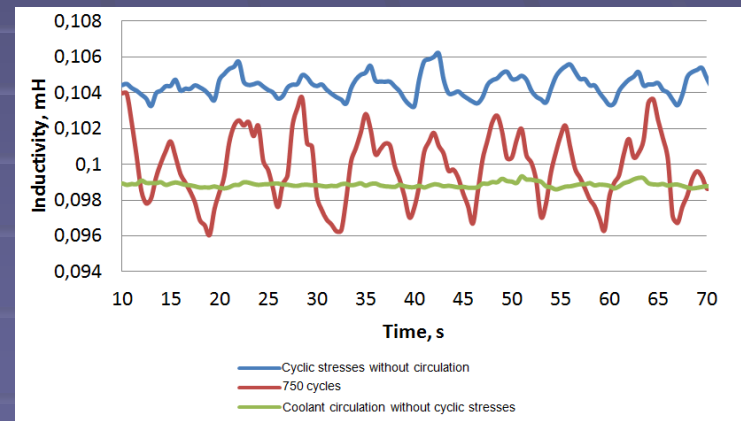
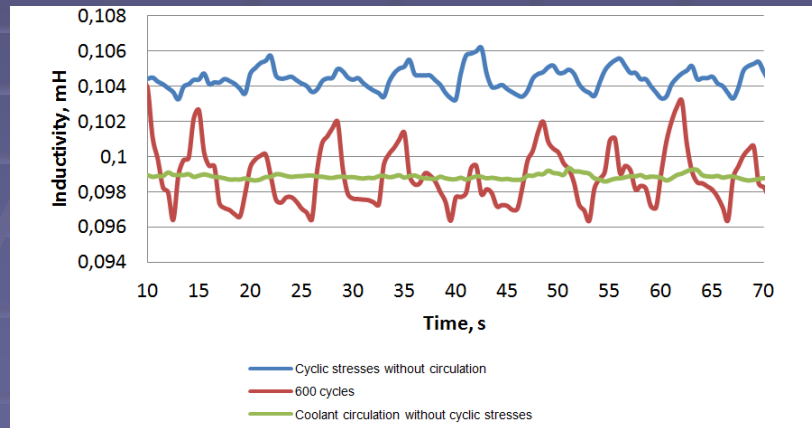
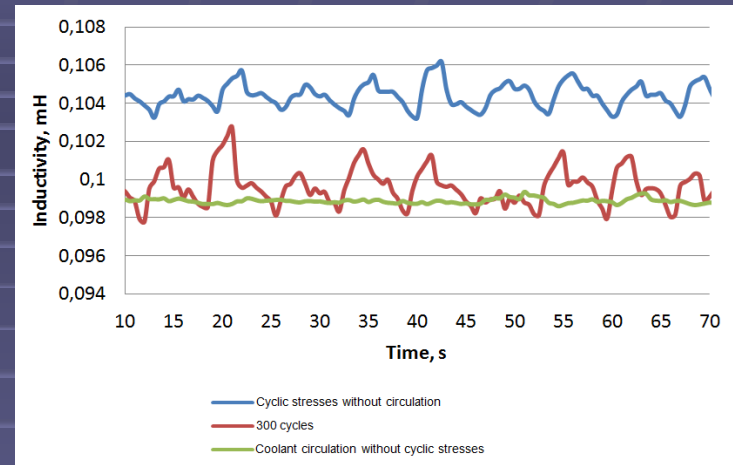
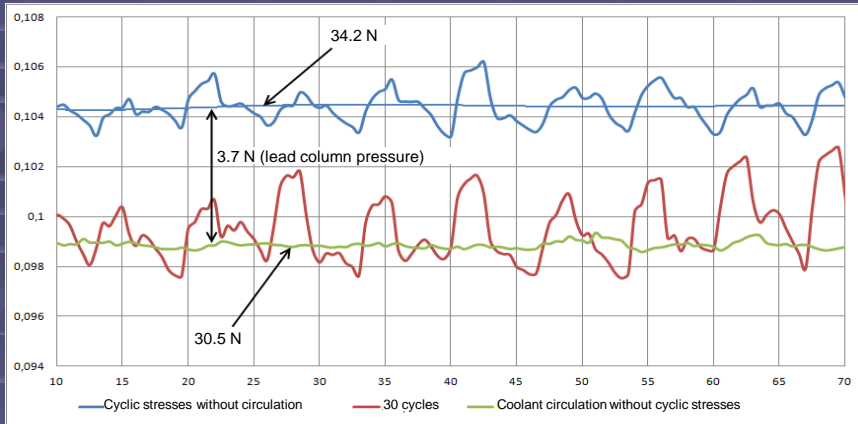


Ra=2.18 μm , Rz=11.05 μm

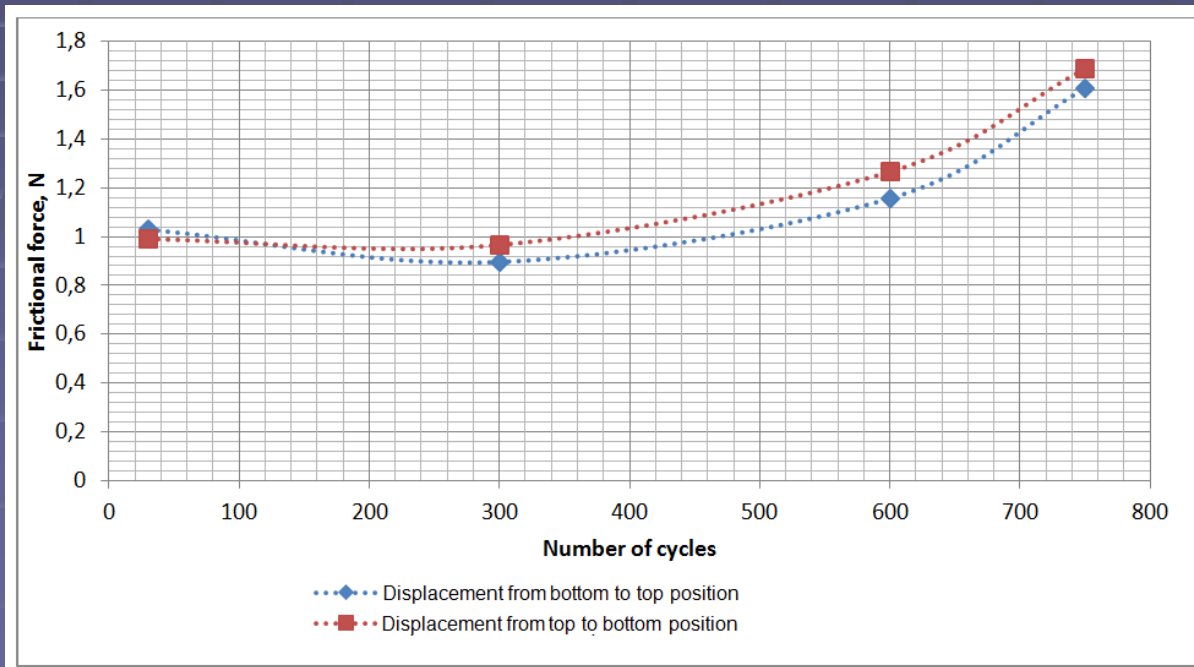
Deterioration without destruction of oxide coatings



Ra=2.131 μm , Rz=9.775 μm



| $P = 668.2L - 35.563$ L - the sensor reading, mH P - the supported force, N | 30 | 300 | 600 | 750 | Without |
|---|--------|--------|--------|--------|-------------|
| | cycles | cycles | cycles | cycles | circulation |
| average amplitude from bottom to top position, N | 32.184 | 32.051 | 32.311 | 32.761 | 34.917 |
| average amplitude from top to bottom position, N | 30.025 | 30.049 | 29.749 | 29.325 | 33.529 |
| average amplitude during cyclic displacements, N | 2.159 | 2.002 | 2.562 | 3.436 | 1.388 |



Conclusions:

1. At the interface of heavy liquid-metal coolants with structural materials, there occurs formation of a wall boundary area whose properties are different from those of the coolants and the structural materials. The properties of this area largely determine the material wear behavior, the hydraulic resistance of the channel and the antifriction properties of the contact area.
2. Solid impurity particles are deposited on the surfaces contacting HLMC in the course of circuit operation, which results in an increase of surface roughnesses. The major parameters affecting the growth of contact surface roughnesses include flow velocity, coolant temperature, thermodynamic activity of oxygen (dissolved oxygen concentration in HLMC), and coolant circulation time, increasing with a rise of these parameters.
3. A wall boundary layer represents a colloid system where impurity particles are a disperse phase, and the coolant itself is a disperse medium. Apparently, viscous properties of such system are different from the "pure" coolant viscosity, which makes it possible to consider such system as a lubricant. The presence of gas (gas-vapor) caverns having linear dimensions ranging from 10 μ m and less in the wall boundary area where HLMC contacts the surfaces of structural materials has been experimentally recorded.
4. Any change in the wall boundary area condition leads to alteration of the tribotechnical characteristics (frictional force and wear rate) of contact surfaces in the system "absorber rod simulator – casing". It was experimentally recorded that the frictional force increased in the context of the experiment due to the coolant flow friction in the annular clearance and the surface contact from 1 N to 1.6 N after 750 cycles of pistonwise displacement. At the same time, surface deterioration was accompanied by destruction of oxide coatings and wetting of contact surfaces with the coolant.